чем сохраняются значения конверсии кислорода, NO_x и ацетилена при умеренных температурах (табл. 5).

Заключение

Компания «Clariant» имеет два типа катализаторов для очистки отходящих газов каталитического крекинга.

1. Никелевый сульфидированный катализатор, применяемый в промышленном масштабе, рекомендуется при нормальных концентрациях CO.

2. Катализатор на основе драгоценного металла предпочтительно использовать для потоков с низким содержанием или отсутствием серы либо при содержании нескольких процентов CO.

Выбор каталитической системы с традиционным никелевым сульфидированным катализатором или с катализатором на основе драгоценного металла в зависимости от состава сырья дает возможность удалить примеси из потоков отходящих газов и таким образом увеличить прибыльность установки крекинга.

UDK 665.753.4:549.67

ON THE WAY TO IMPROVE CETANE NUMBER IN DIESEL FUELS: RING OPENING OF DECALIN OVER IR-MODIFIED EMBEDDED MESOPOROUS MATERIALS

© 2013 г. **N. Kumar**[1], **P. Mäki-Arvela**[1], **N. Musakka**[1], **D. Kubicka**[1], **M. Kangas**[1], **M. Tiitta**[2], **H. Österholm**[2], **A.-R. Leino**[3], **K. Kordás**[3], **T. Heikkilä**[4], **T. Salmi**[1], **D.Yu. Murzin**[1]

[1] Laboratory of Industrial Chemistry and Reaction Engineering, Department of Chemical Engineering, Process Chemistry Centre, Åbo Akademi University, FI-20500 Turku/Åbo, Finland

[2] Neste Oil, Technology Center, P.O.B. 310, FI-06101 Porvoo, Finland

[3] Laboratory of Microelectronics and Materials Physics, University of Oulu, PL 4500, FI-90014 Oulu, Finland

[4] Laboratory of Industrial Physics, University of Turku, FI-20014 Turku, Finland

1. Introduction

Microporous acidic zeolite catalysts have been applied in several industrial processes of oil refining, fine chemicals and environmental catalysis. However, due to the size of micropores, there are diffusion limitations for processing large molecules. Hence, there is need for the development of large pore size, active and selective mesoporous material catalysts, possessing strong acidity and high hydrothermal stability. The development of M41S mesoporous materials in 1992 by Mobil Corporation [1] was a breakthrough in the direction of preparing mesoporous materials which can be applied in the reactions involving large size reactants and reaction products. These mesoporous materials with large pore size and minor diffusion limitations, exhibited only mild acidity. They were hydrothermally less stable than zeolites and deactivated rapidly in oil refining processes.

Synthesis of embedded micro-mesoporous materials has been an important research area in order to combine the benefits of the mesoporous materials and the high acid site concentration in zeolites [2, 3]. A recent review describes different techniques to synthesize micro-mesoporous materials [2]. One method is to synthesize mesoporous materials embedded with zeolite via sequential synthesis of colloids of for example zeolite beta and adding viscous gel of tetracetyl ammonium bromide forming MCM-41 [4]. Zeolite seeds were also added in the gel solution of the mesoporous phase MCM-41 [5]. The embedded mesoporous materials have high hydrothermal stability, exhibit strong Brønsted and Lewis acidity and are coke resistant for processing of large size molecules [2]. Furthermore, it is possible to design and vary the amounts of Brønsted and

Lewis sites in these mesoporous materials.

Production of high quality environmental friendly diesel fuel is important from the viewpoint of economy, environment and human health. One of the targets for the fuel producing companies is to decrease the sulphur and aromatics contents in the middle distillates or some other streams to produce high quality diesel fuel with improved cetane number. For example Light Cycle Oil does not meet current diesel specifications, containg high amounts of polyaromatics (*ca*. 48—69 %) and pocessing low cetane number (*ca*. 18—25). The latter should be increased to at least 51. Hydrotreating of aromactics improves cetane index, although this increase is not sufficient, and a ring opening of naphthenic compounds is needed. During this process the cetane number increases when compounds with two naphthenic rings undergo transformations into linear or mono-branched paraffins. One of the most challenging and catalytically viable pathways is to perform ring opening of such compounds selectively.

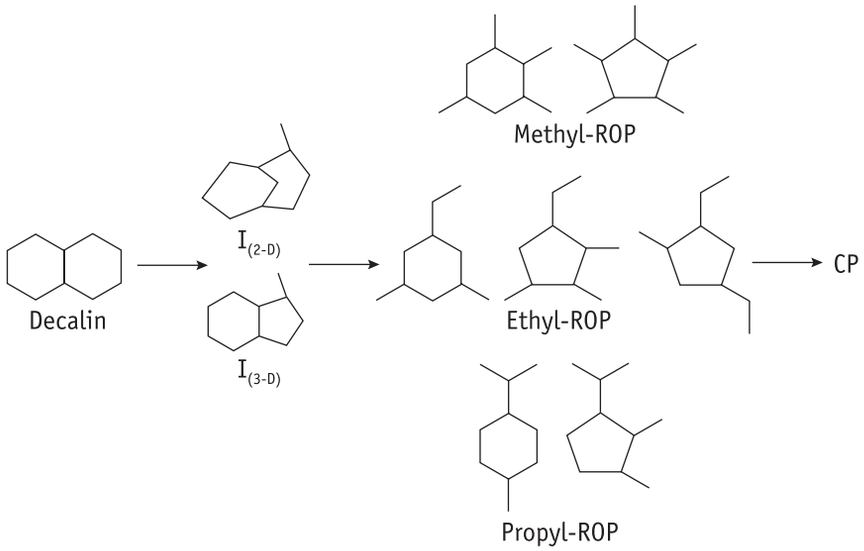

Fig. 1. Reaction scheme for ring opening of decalin

I – isomers, ROP – ring opening products, CP – cracking products containing less than 10 carbon atoms

Ring opening of decalin has been discussed in several papers [6—21] over different types of catalysts, for example over Pt- and Ir-modified zeolite and aluminum oxide catalysts [3—7], recently also Ir- and Pt-supported on La-X zeolite [11] and Rh/H—BE [12] have been applied as catalysts in gas-phase ring opening of decalin. Bi-metallic Pt-Ir-modified MCM-41, mesoporous material, was investigated for selective ring opening of decalin [13], ring opening and hydrogenation of tetralin was studied over Ni- and NiMo-supported over alumina-pillared zirconium phosphate catalysts [15]. Furthermore, Ir-Pt and NiMo carbide catalyst supported on zeolites were studied in ring opening of decalin [14].

The following mechanism for ring opening of decalin has been proposed over Pt-modified zeolites as follows: the reaction starts with dehydrogenation and protonation followed by protolytic dehydrogenation and cracking. Thereafter the reaction proceeds via skeletal isomerization, hydride transfer, olefin adsorption-desorption and hydrogenation. Ring opening proceeds further via β-scission followed by consecutive hydrogenation and opening of the ring finally via hydrogenolysis. Large molecules can still be alkylated and thus coke can be formed [4]. The products formed in the ring opening of decalin were classified in [4] in four groups being *trans*-decalin, other isomerization products (I), ring opening products (ROP) and cracking products (CP). The isomers denote C10 bicyclic compounds, whereas ring opening products were C10 containing monocyclic compounds, such as tetramethylcyclohexanes, methyl-propylcyclohexanes, butylcyclohexanes, diethyl-cyclohexanes and ethyl-trimethylcyclopentanes [7]. Cracking products were defined as products with a lower molecular weight compared to that of decalin [7] (Fig. 1). The selectivity to ring opening products in-

Narendra Kumar *– Ph.D., senior researcher, Laboratory of Industrial Chemistry and Reaction Engineering, Department of Chemical Engineering, Process Chemistry Centre, Åbo Akademi University, FI-20500 Turku/Åbo, Finland*

Päivi Mäki-Arvela *– Ph.D., lecturer, the same laboratory*

Niko Musakka *– Ph.D., researcher, the same laboratory*

David Kubicka *– Ph.D., researcher, the same laboratory*

Matias Kangas *– Ph.D., researcher, the same laboratory*

Marja Tiitta *– Ph.D., researcher, Neste Oil, Technology Center, P.O.B. 310, FI-06101 Porvoo, Finland*

Heidi Österholm *– M.Sc., researcher, the same center*

Anne-Riikka Leino *– M.Sc., researcher, Laboratory of Microelectronics and Materials Physics, University of Oulu, PL 4500, FI-90014 Oulu, Finland*

Krisztian Kordás *– senior researcher, the same laboratory*

Teemu Heikkilä *– MSc, researcher, Laboratory of Industrial Physics, University of Turku, FI-20014 Turku, Finland*

Tapio Salmi *– Ph.D., Professor, Laboratory of Industrial Chemistry and Reaction Engineering, Department of Chemical Engineering, Process Chemistry Centre, Åbo Akademi University, FI-20500 Turku/Åbo, Finland*

Dmitry Yu. Murzin *– Dr.Sc., Professor, the same laboratory.*
Ph: +358 2 215-49-85, fax: +358 2 215-44-79. E-mail: dmurzin@abo.fi

creased with increasing conversion and the intermediate isomer compounds showed a maximum in their product distribution [7]. Furthermore, it has been suggested that ring opening of C10 napthenes occurs over acid sites via carbocations and via hydrogenolysis over noble metals simultaneously [8]. The maximum selectivity of ring opening products over 2 wt.% Pt-H-BE has been 30 % at an optimum temperature of 523 K at 2 MPa [7]. More recently a detailed analysis of the isomer structures has been provided [12] in which the ring opening of decalin was studied over Pt-H-BE zeolite. The results showed that both planar 2-D and non-planar 3-D can be formed (Fig. 1). Furthermore, it was concluded that 2-D isomers, such as methylbicyclo (4.3.0) nonane and dimethylbicyclo (3.3.0) octane, are more important in the decalin ring opening than the 3-D isomers. Interestingly, an increase in concentration with increasing temperature was only observed for 3-D isomers, e. g. methylbicyclo (3.3.1) nonane, dimethylbicyclo (3.2.1) octane and trimethylbicyclo (2.2.1) heptane.

Selective ring opening of decalin has been recently studied over Pt/La-X and Ir/La-X in gas phase at 528 K under 5.2 MPa total pressure [11]. Due to the use of 2D-GC analysis method and by synthesizing model compounds, such as iso-decanes it was possible to identify and quantify so called open chained decanes with the molecular formula of $C_{10}H_{22}$, (M_w = 142 g/mol) in the product mixture from the ring-opening of decalin [11]. Ring opening products in the work of Rabl et al. [11] were defined as $C_{10}H_{20}$ with the molecular mass of 140 g/mol. The selectivity to ring opening products was about 30 % at 92 % conversion over Pt/La-X at 523 K. Furthermore, the existence of spiro (4.5) decane, bicycle (4.3.1) decane and bicycle (5.3.0) decane was confirmed using gas chromatography-mass spectrometry (GC-MS) together with GC and nuclear magnetic resonance spectroscopy (NMR). It was proposed in [11] that spiro (4.5) decane can be formed from carbenium ions in decalin, whereas 1, 2-alkyl shift could start from tertiary or secondary carbenium ion forming bicycle (4.3.1) decane or bicycle (5.3.0) decane, respectively.

In this paper, Ir-modified MCM-41 embedded either with BE or TON zeolites were synthesized and characterized using such methods as X-ray powder diffractometry (XRD), scanning electron microscopy (SEM), wavelength dispersive X-ray fluorescence spectroscopy (XRF), high resolution transmission electron microscopy (HR-TEM), nitrogen adsorption and infrared spectroscopy of pyridine (Py-FTIR). The performance of these catalysts was studied in ring opening of a model compound — decalin. The main parameters in the catalytic tests were temperature and pressure. Furthermore, the roles of iridium and Brønsted acid sites on the conversion of decalin and selectivity to ring opening products were explained together with the influence of zeolite structure of the embedded mesoporous material. Results from the physico-chemical characterization of proton and iridium modified embedded mesoporous material catalysts have been correlated with catalytic data for the ring opening of decalin.

2. Experimental

2.1. Synthesis and characterization of Ir-modified H-NK-MM-BE and H-NK-MM-TON embedded mesoporous materials

Na-NK-MM-BE and Na-NK-MM-TON parent forms of embedded mesoporous materials were synthesized by preparing BE and TON zeolite structure nuclei and introducing it in a gel solution of mesoporous material. The mesoporous material gel solution containing BE and TON nuclei was introduced in two separate Teflon cups, which were then introduced in 300 ml autoclaves (Parr). After completion of synthesis the autoclaves were quenched in a water bath, crystalline products filtered and washed thoroughly in a flow of distilled water. The embedded mesoporous materials were recovered from the filter paper and dried in ceramic plates at 373 K, followed by calcination in a muffle oven using step calcination procedure. Na-NK-MM-BE and Na-NK-MM-TON mesoporous materials were transferred to H-NK-MM-BE and H-NK-MM-TON by ion-exchange method using 1M ammonium nitrate aqueous solution for 24 h at ambient temperature. After ion-exchange NH_4-NK-MM-BE and NH_4-NK-MM-TON mesoporous materials were washed free of chloride ions using distilled water, followed by drying at 373 K and calcination in a muffle oven using step calcination procedure to obtain H-NK-MM-BE and H-NK-MM-TON catalysts.

2 wt.% Ir-H-NK-MM-BE and 2 wt.% Ir-H-NK-MM-TON embedded mesoporous material catalysts were prepared by evaporation impregnation method using an aqueous solution of iridium chloride in a Buchi rotator evaporator. Ir modified mesoporous material catalysts were dried at 373 K and *in situ* pretreatment with hydrogen or oxygen was carried out in an autoclave 300 ml (Parr) reactor while testing the catalysts in ring opening reaction of decalin. The detailed procedure is reported in [5].

Na-NK-MM-BE, Na-NK-MM-TON, H-NK-MM-BE, H-NK-MM-TON, 2 wt.% Ir-H-NK-MM-BE and 2 wt.% Ir-H-NK-MM-TON mesoporous material catalysts were characterized by using different methods. The XRD analyses were made by X'Pert High Score Software (Phi-

lips, 2001) and the powder diffraction data base (PDF-2, 1996 release ICDD) was used to identify crystalline compounds. Furthermore, the unit cell dimension (a_0) for MCM-41 was estimated by the equation $a_0 = 2d_{[100]}/\sqrt{3}$ [1]. The a_0 for BE was estimated from the [302] reflection at 22° 2θ with a modified ASTM D 3942-97 method using TiO_2 as an internal standard.

SEM (Leo 360) was applied for determination of morphology (shape, size and distribution of crystals), the specific surface area of the catalysts were measured with nitrogen adsorption using Sorptometer 1900 (Carlo Erba Instruments). Prior to the measurements the samples were evacuated at 423 K for 3 h.

The quantitative measurements of the Brønsted and Lewis acid sites in the proton and Ir-modified A and B embedded mesoporous materials were performed using FTIR (ATI Mattson Infinity Spectrometer) and pyridine (99.5 %) as a probe molecule. A self supported wafer (10—12 mg/cm^2) was prepared and pyridine was adsorbed at 373 K for 30 min, followed by desorption at 523 K, 623 K and 723 K. The Brønsted and Lewis acid sites were calculated from the peaks at the spectral bands at 1545 cm^{-1} and 1450 cm^{-1}, respectively. The quantification of the adsorbed pyridine was performed using the molar extinction coefficient from [22].

The quantitative analysis of Si and Al was made by wave length dispersive X-ray fluorescence spectrometry (XRF), with Bruker S4 instrument. The samples were first dried at 393 K for 2 h, then humidified for at least 16 h over water saturated with $CaCl_2 \cdot H_2O$. The humidification minimized variations in moisture content and allowed a careful sample weighing. The XRF samples were prepared from 500 mg sample, mixed with Li-tetraborate to 10 g total weight. Fused glass beads were made under mixing at 1623 K and thereafter cooled in special molds under controlled conditions. The solid solutions with a perfect sample surface were found to be the most reliable quantitative method for this type of materials.

TEM was used for investigation of the phase purity, long range ordering and periodicity. The mean Ir-particle sizes were calculated based on the frequency of particles from images obtained by a LEO 912 OMEGA energy-filtered transmission electron microscopy (TEM) operating with acceleration voltage of 120 kV. At least 100 particles were counted for obtaining average particle diameter of Ir.

2.2. Experimental procedure for ring opening of decalin

Ring opening of decalin was carried out in a 300 ml stainless steel autoclave (Parr Industries), which was connected to a temperature controller and a pressure regulator. The Ir-modified embedded mesoporous catalysts were pre-treated *in situ* in presence of hydrogen prior to the catalyst testings via reducing the catalyst with the following temperature program: 3 K/min — 623 K (10 min). The catalysts were crushed and sieved; and fraction below 63 μm was used in the catalyst testing which along with efficient stirring (1500 r/min) prevented internal and external mass transfer limitations. The reaction temperature and pressure were varied in the range of 523—623 K and 2—6 MPa, respectively. The reactant used for the testing of embedded mesoporous catalysts consisted of a mixture of decalin (bicycle (4.4.0) decane) isomers (Fluka, 98 %) with a *cis* to *trans* ratio of 0.66. In a typical experiment 50 g deoxygenated reactant was injected into the reactor containing about 1 g of catalyst. Thereafter the reactor was pressurized with hydrogen (99.999 %), temperature and pressure were increased to the desired level. Due to the small changes in the catalyst and reactant amounts in different experiments the results depicting the comparisons of different experiments are shown by plotting as x-axis instead of reaction time, a normalized time, being time multiplied by mass of decalin divided by mass of catalysts.

The product analysis was carried out by using a gas chromatograph (Agilent 6890N) equipped with a capillary column (DB-Petro, 50 mm × 0.2 mm × 0.5 μm) and a FI detector. Initial product identifications were carried out by a GC/MS (HP 6890-5973) instrument. The details of analysis can be found in reference [9]. It should be pointed out here that the grouping of different products (isomers, ROP, CP) was made according to the definition of the yields of isomers, ROP and CP products according to [7] without taking into account any open chain decanes, which have been recently identified in [11].

3. Results and discussions

3.1. Catalyst characterization results

The X-ray powder diffraction patterns of Na-NK-MM-BE and Na-NK-MM-TON embedded mesoporous materials exhibited two phases: mesoporous material phases at low angle peaks of 2θ values of 0.2° to 8° followed by zeolitic phases. The zeolitic phases obtained for Na-NK-MM-BE and Na-BE embedded mesoporous materials were typical of those found for the BE and TON type zeolite structures. X-ray powder diffraction patterns of Na-NK-MM-BE and 2 wt.% Ir-NK-MM-TON embedded mesoporous material are given in Fig. 2 and Fig. 3, respectively. The hexagonal structure of MCM-41 was clearly visible in the Miller

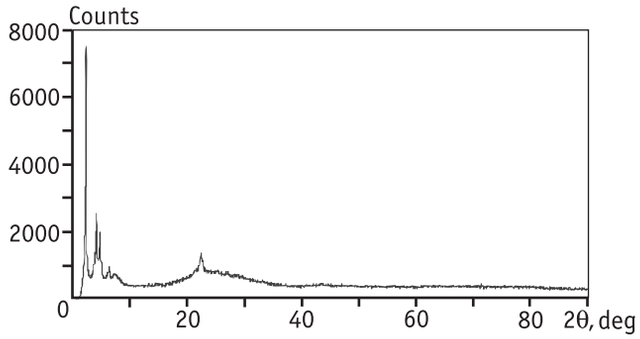

Fig. 2. X-ray powder diffraction pattern of Na-NK-MM-BE embedded mesoporous material

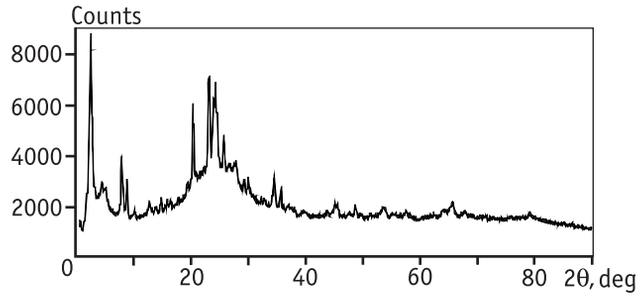

Fig 3. X-ray powder diffraction pattern of 2 wt.% Ir-H-NK-MM-TON embedded mesoporous material

indexes (100), (110), (200) and (220) which exhibited the 2θ values of 2, 3.8, 4.2 ad 5.8, respectively according to [23], whereas the most intense peaks for Na—BE in the diffractogram are visible at 2θ of 22.4° and 7.6°, respectively analogously to [3, 4, 24]. It is noteworthy to mention here that there were no other zeolitic phases, than BE and TON, clearly indicating the high phase purity of the embedded mesoporous materials. The unit cell dimension a_0, for MCM-41 and for BE in Na-NK-MM-BE embedded micro-mesoporous material were according 4.0 nm and 1.428 nm, respectively, whereas for the pure MCM-41 it was 2.5—3.0 nm [5].

Ir-modified H-NK-MM-BE and H-NK-MM-TON mesoporous materials were also characterized with X-ray powder diffraction method. The X-ray powder diffraction patterns of 2 wt.% Ir-NK-MM-BE and 2 wt.% Ir-NK-MM-TON were similar to those of parent Na-NK-MM-BE and Na-NK-MM-TON mesoporous materials with extra peaks at 2θ values of 28, 34.8 and 40°, which were attributed due to presence of IrO_2. It was inferred from this analysis result that the introduction of Ir to the embedded mesoporous materials did not influence the parent structures of MM-BE and MM-TON. It was further concluded from this result that the method and synthesis conditions applied for the preparation of Ir-modified catalysts were appropriate.

Scanning electron micrographs of Na-NK-MM-BE exhibited crystals of BE zeolite structure phase (separate circular shaped crystals and agglomerates), mesoporous material (bead shape) and mixed phases of BE zeolite and mesoporous materials. Scanning electron micrographs of Na-NK-MM-BE confirms the embedding of BE zeolite structure to the mesoporous material. Scanning electron micrographs of Na-NK-MM-BE and Na-NK-MM-TON embedded mesoporous materials are given in Fig. 4 and Fig. 5, respectively. Scanning electron micrographs of Na-NK-MM-TON embedded mesoporous material showed TON zeolite structure (separate needle shape crystals and agglomerates), mesoporous material (bead shape) and also mixed phases of TON zeolite structure and mesoporous material. Further indication for synthesis of a mesoporous material embedded with a TON type zeolite structure and mesoporous material (picture not depicted here).

The H-NK-MM-TON embedded mesoporous material catalyst exhibited about the same concentration of weak Brønsted (temperature — 523 K) and Lewis acid sites as being present in the 2 wt.% Ir-modified H-NK-

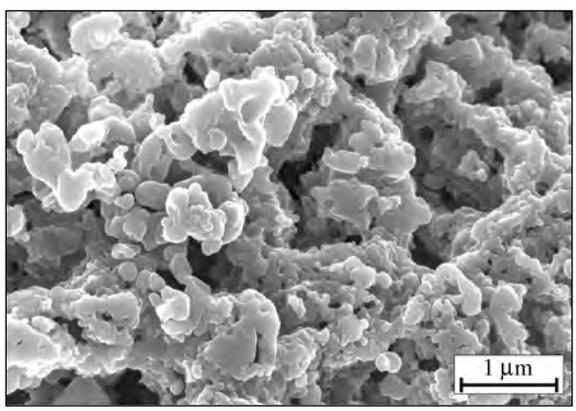

Fig. 4. Scanning electron micrograph of Na-NK-MM-BE embedded mesoporous material

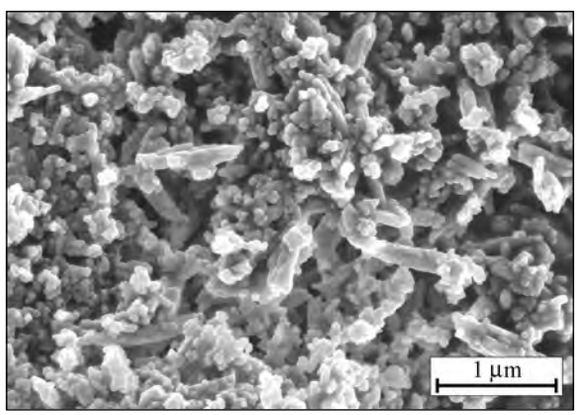

Fig 5. Scanning electron micrograph of Na-NK-MM-TON embedded mesoporous material

Table 1

Determination of Brønsted and Lewis acid sites in Ir- and H-forms NK-MM-BE and NK-MM-TON embedded mesoporous materials using FTIR of pyridine

Catalyst	Al, wt.% (Si/Al)	Brønsted acid sites, μmol/g, at desorption temperature, K			Lewis acid sites, μmol/g, at desorption temperature, K		
		523	623	723	523	623	723
2 wt.% Ir-H-NK-MM-BE	1 (40.4)	95	32	8	58	5	3
2 wt.% Ir-H-NK-MM-TON	2 (20.8)	102	32	0	59	1	0
H-NK-MM-TON	2 (20.8)	89	65	22	50	25	6

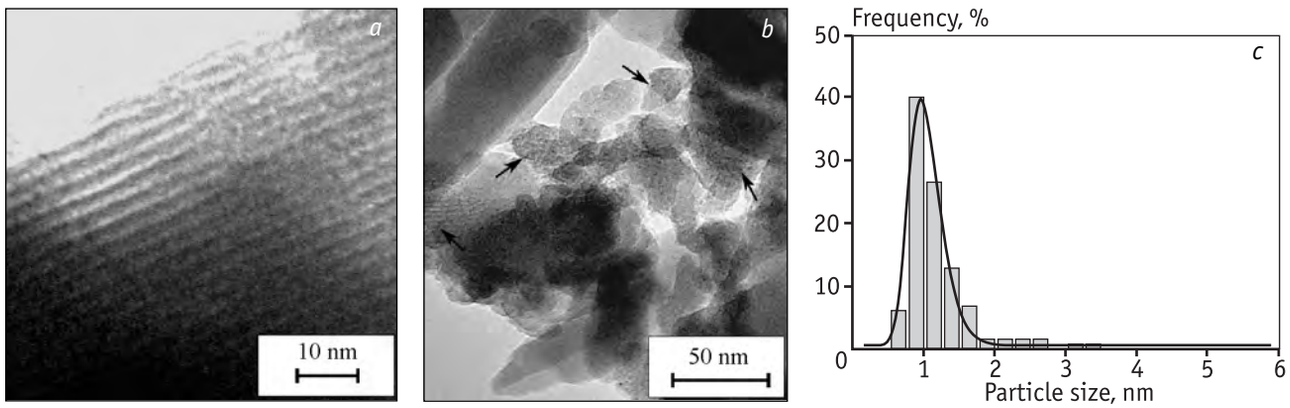

Fig. 6. TEM images of 2 wt.% Ir-H-NK-MM-TON embedded mesoporous material (*a, b*) and the Ir-particle size distribution (*c*)

MM-TON catalyst (Table 1). However, the amounts of medium and strong Brønsted (corresponding to pyridine desorption at 623 and 723 K) and Lewis acid sites were higher in H-NK-MM-TON than those in 2 wt.% Ir-H-NK-MM-TON catalyst. A slight increase in the Brønsted and Lewis acid sites of 2 wt.% Ir-modified H-NK-MM-TON catalyst may be attributed to the interaction of support (embedded mesoporous material) and iridium metal particles or influence by $IrCl_3$ during impregnation. A higher amount of total Brønsted acid sites was present in the 2 wt.% Ir-H-NK-MM-TON embedded mesoporous catalyst than in 2 wt.% Ir-H-NK-MM-BE. This result is expected due to higher amount of Al present in the framework of the Ir-H-NK-MM-TON compared to Ir-H-NK-MM-BE. However, the amount of strong Brønsted acid sites (723 K) in 2 wt.% Ir-H-NK-MM-BE was higher than that of 2 wt.% Ir-H-NK-MM-TON catalyst, being still much less than for non-modified catalyst. Metal-support interactions and their influence on the physico-chemical and catalytic properties is a well known phenomenon in catalysis. Observations of alterations of the strength of acid sites have been also reported previously in the literature for other metal modified zeolites. For example influence of Pt-particles on the acidic properties of BE and MOR zeolites previously reported in [7], based on the acidity measurements, catalytic data and various physico-chemical methods, showing that introduction of metal significantly diminished the presence of strong sites, which in turn decreased cracking abilities of platinum catalysts supported on zeolites in the same reaction of decalin ring opening. These observations are in line with the data in the current work.

TEM images and Ir-particle size distributions for Ir-H-NK-MM-TON and Ir-H-NKK-MM-BE are depicted in Fig. 6 and 7. The average Ir-particle diameter in H-NK-MM-TON was 1.3 nm, which is lower than that of Ir in H-NK-MM-BE embedded mesoporous material being 2.1 nm (Table 2, Fig. 6, *c* and 7, *b*). The Ir-particle size (Fig. 7, *b*) distribution 2 wt.% Ir-H-NK-MM-BE was also broader than that of 2 wt.% Ir-H-NK-MM-TON. The one-dimensional structure of zeolite ZSM-22 with TON topology, has the pore size of 0.57 nm × 0.46 nm [25] and thus the narrow Ir-particle size distribution can be expected, whereas there are more possibilities to obtain large Ir-particles in the three-dimensional H-BE structure. The TEM images showed that pore structure of H-NK-MM-BE and H-BE embedded mesoporous materials is well defined and uniform (Fig. 7, *a*). The transmission elec-

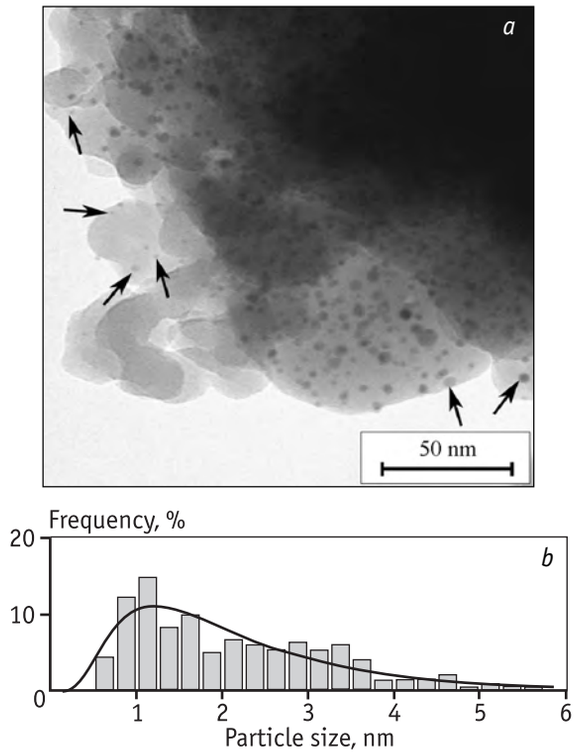

Fig. 7. TEM image of Ir-H-NK-MM-BE embedded mesoporous material (*a*) and the Ir-particle size distribution (*b*)

Table 2

Determination of Ir dispersion and Ir particle diameter in 2 wt.% Ir-H-NK-MM-BE and 2 wt.% Ir-H-NK-MM-TON catalysts using CO pulse chemisorption

Catalyst	Ir dispersion, %	Average Ir diameter, nm
2 wt.% Ir-H-NK-MM-BE	30	3.7
2 wt.% Ir-H-NK-MM-TON	29	3.9

tron micrograph of 2 wt.% Ir-H-NK-MM-TON exhibits also an ordered mesoporous structure (Fig. 6, *a*). The high surface area (734 m^2/g) obtained for the embedded mesoporous material confirms the presence of ordered mesoporous structure. However, there may occur some disordering in the embedded mesoporous material structure during the modification with aqueous solution of $IrCl_3$.

The surface areas of H-NK-MM-BE, H-NK-MM-TON, 2 wt.% Ir-H-NK-MM-BE and 2 wt.% Ir-H-NK-MM-TON catalysts were measured by nitrogen adsorption, and calculated with the BET method. The surface areas were determined to be 1013, 731, 1145 and 734 m^2/g, respectively. Furthermore the mesopore diameter was in a range of 2.4 to 2.7 nm in H-NK-MM-BE [5]. Enhancement in surface area is due to the formation of micropores during calcination. In addition, impregnation can also influence the surface area.

3.2. Ring opening of decalin over 2 wt.% Ir-H-NK-MM-BE, 2 wt.% Ir-NK-MM-TON and H-NK-MM-TON embedded mesoporous materials

3.2.1. Overall kinetics in decalin transformation. Ring opening of decalin has a complex reaction network, in which three kinds of products, namely isomers of decalin, ring opening products (ROP), cracking products (CP) as well as heavy compounds are formed. The CPs contain less than 10 carbon atoms, whereas heavy products have more than 10 carbon atoms. Typical isomers are different methylbicyclononanes, dimethylbicyclooctanes, trimethylbicycloheptanes etc. ROPs consist of cyclohexyl or cyclopentyl-derivatives containing methyl-, propyl- and butyl-side chains. Over Pt-modified zeolites, the first reaction step is the formation of isomers followed by generation of ROPs and CPs in the second and third steps, respectively [7]. In the current case of Ir-supported on hybrid materials consisting of mesoporous MCM-41 and BE zeolite structures, namely in 2 wt.% Ir-H-NK-MM-BE, the decalin transformation was relatively fast, i. e. above 70 % of decalin was transformed within 180 min. The ratio between the initial rates for the formation of isomers, ROPs and CPs after 30 min was 66 : 2.5 : 1 and thus the main primary products were isomers. The formation rate of ring opening products was enhanced by factor 1.6 after 90 min of reaction time compared to their initial formation rate, indicating that ROPs were mainly formed in the consecutive step. Furthermore, at the end of the reaction also some heavy products were observed, being maximally about 2.7 mol.% of the reaction mixture at 98 % conversion. The selectivity to ROP at this conversion level was about 35 % maximum.

3.2.2. Effect of structure of H-NK-MM-BE and H-NK-MM-TON embedded mesoporous materials on conversion of decalin and selectivity to ring opening products. A comparison of two support structures on the ring opening of decalin has been performed with 2 wt.% Ir-H-NK-MM-BE and 2 wt.% Ir-H-NK-MM-TON embedded mesoporous materials at 6 MPa and 573 K (Fig. 8, Table 3, entries 2 and 6). The initial rate of 2 wt.% Ir-H-NK-MM-BE was 32 fold compared to that of 2 wt.% Ir-H-NK-MM-TON. The ratio of the initial formation rates of the isomers, ROP and CP products after 30 min was 9.4 : 2.2 : 1 over 2 wt.% Ir-H-NK-MM-TON indicating that the formation of isomers was much slower compared to the case using 2 wt.% Ir-H-NK-MM-BE as a catalyst (see

Table 3

Experimental data in decalin transformation over 2 wt.% Ir-H-NK-MM-BE, 2 wt.% Ir-H-NK-MM-TON and H-NK-MM-TON embedded mesoporous materials

Entry	Catalyst	Temperature, K	Pressure, MPa	Initial reaction rate, mmol/min/$g_{cat.}$	Conversion after 20 min normalized time, %	Selectivity, %, to			
						ROP at 30 % conversion	isomers at 30 % conversion	cracking products at 30 % conversion	ROP at 90 % conversion
1	Ir-H-NK-MM-BE	523	6	0.08	28	7	96	2	16
2	Ir-H-NK-MM-BE	573	6	2.3	91	4	99	3	28
3	Ir-H-NK-MM-BE	623	6	5.6	98	–*	86*	8*	–**
4	Ir-H-NK-MM-BE	573	2	2.0	80	7	10	5	17
5	Ir-H-NK-MM-BE	573	4	2.0	91	4	10	5	13
6	Ir-H-NK-MM-TON	573	6	0.07	22.5	28	58	6	–**
7	H-NK-MM-TON	573	6	0.05	15	4***	84***	8***	–**

* The lowest conversion measured was 42 %.
** Not 90 % conversion reached.
*** Conversion level of 17 %.

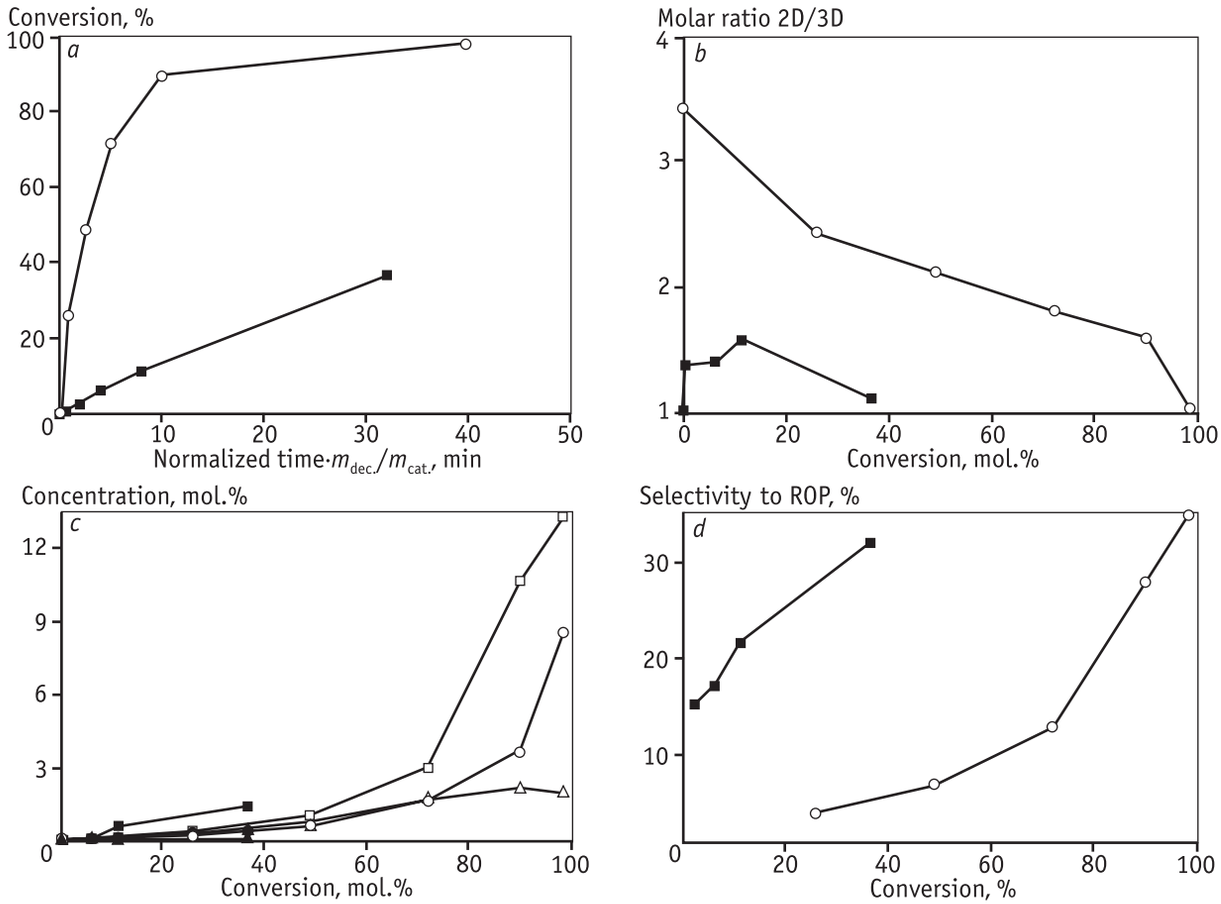

Fig. 8. Effect of structure on conversion of decalin (*a*), molar ratio of 2D to 3D isomers (*b*), concentration of ROP (*c*) and selectivity to ring opening products as a function of conversion (*d*) in decalin ring opening reaction at 573 K and 6 MPa

Symbols (*a, b, d*): ○ – 2 wt.% Ir-H-NK-MM-BE, ■ – 2 wt.% Ir-H-NK-MM-TON

Symbols (*c*): ○ – methyl ROP, □ – ethyl ROP, △ – propyl ROP; open symbol – Ir-H-NK-MM-BE, solid symbol – Ir-H-NK-MM-TON

Section 3.2.1). In addition, the conversion of decalin over 2 wt.% Ir-H-NK-MM-BE catalyst was about 93 % with the normalized time of 34 min, whereas the corresponding conversion with 2 wt.% Ir-H-NK-MM-TON was only 32 % (Fig. 8, *a*). The conversion increased continuously over both catalysts and thus the catalysts were active after prolonged reaction times. The higher reaction rates achieved by 2 wt.% Ir-H-NK-MM-BE compared to 2 wt.% Ir-H-NK-MM-TON, which contain embedded BE and TON zeolites, respectively, can be explained by the fact that there are large differences in the their pore sizes. In the catalyst 2 wt.% Ir-H-NK-MM-BE the zeolite phase is BE, which has three dimensional channel systems with one 12-membered ring channels in C-direction having pores with 0.67×0.66 nm, another two channels in a direction perpendicular to C-direction with pores 0.67×0.66 nm and 0.56×0.56 nm. In 2 wt.% Ir-H-NK-MM-TON catalyst the zeolite phase is ZSM-22, which has TON topology and narrow pore structure (see Section 3.1) [27]. On the other hand, the particle size of 2 wt.% Ir-H-NK-MM-BE was even larger than that for 2 wt% Ir-H-NK-MM-TON thus indicating that the metal particle size did not affect very much the reaction rate.

Comparing performance of 0.98 wt.% Ir-H-MCM-41 mesoporous material and 2 wt.% Ir-H-NK-MM-BE embedded mesoporous material, it can be observed that the hybrid material was more active in the decalin conversion at 623 K. The Ir-MCM-41 mesoporous catalyst converted about 60 % of decalin in 360 min [20], whereas 2 wt.% Ir-H-NK-MM-BE embedded mesoporous material was able to transform about 96 % of decalin within 360 min at 623 K and 6 MPa. It should be pointed out that the pressure has only a minor effect on decalin conversion (see Section 3.2.5). The acidity of the parent H-MCM-41 mesoporous material was very low [7], which mainly explains the lower conversion obtained with 0.98 wt.% Ir-H-MCM-41 compared to the 2 wt.% Ir-H-NK-MM-BE embedded mesoporous material.

The product distributions using 2 wt.% Ir-H-NK-MM-BE or 2 wt.% Ir-H-NK-MM-TON embedded mesoporous materials differed for extended reaction times. For 2 wt.% Ir-H-NK-MM-BE isomers formation was rapid and their amount exhibited a maximum level about 58.5 mol.% at 5 min normalized time, whereas only about 26 % isomers were maximally formed with 2 wt.% Ir-H-NK-MM-TON catalyst after 1440 min. The ring opening of decalin has been stated to occur via its isomerization followed by the ring opening *per se* [7]. The isomers formed can either be two dimensional or three dimensional [16]. Thus the ratio between 2D and 3D isomers was plotted as a function of decalin conversion (Fig. 8, *b*) and the results showed that this ratio was much lower over 2 wt.% Ir-H-NK-MM-TON than over 2 wt.% Ir-H-NK-MM-BE. Furthermore, the 2D to 3D ratio decreased with increasing conversion. This result can be explained by the fact that 2D isomers are formed via a dehydrogenation route. Initially, formation rate of 2D isomers was about 2.5 fold compared to the formation rate of the 3D isomers over 2 wt.% Ir-H-NK-MM-BE. In addition, their concentrations reached a maximum value at the same time and thus it cannot be directly concluded from kinetic data that 3D isomers would be formed from 2D isomers. On the other hand, the difference in the formation rates of 2D and 3D isomers over H-NK-MM-TON catalyst was not as large as in case of H-NK-MM-BE and maximum concentrations of isomers were not reached in the studied time period. Since the 2D to 3D ratio decreased with increasing concentration, it can be assumed that 2D isomers reacted relatively rapidly to ring opening products, whereas 3D isomers react to heavy compounds.

ROP products are mainly formed from 2D decalin isomers and their amount was also about 9.6 mol.% after 1440 min over 2 wt.% Ir-H-NK-MM-TON. This amount was only about 28 % of the formed amount of ROP obtained over 2 wt.% Ir-H-NK-MM-BE embedded mesoporous material. The detailed distribution of ring opening products is shown in Fig. 8, *c*. The results showed that the main products over embedded mesoporous catalysts were ring opening products containing an ethyl side chain, for example diethyl cyclohexanes, ethyl-trimethyl cyclopentanes and diethyl methyl cyclopentanes. This result deviates from the one achieved in decalin ring opening over microporous Pt-H-BE catalysts, over which the main ring opening products were composed of methyl chain ring opening products, such as tetramethyl cyclohexanes and pentamethyl cyclopentanes [17]. This difference can originate either from the different metal used or different pore structures. The difference in 2 wt.% Ir-H-NK-MM-TON and 2 wt.% Ir-H-NK-MM-BE embedded mesoporous material was minor in the distribution of ring opening products. The second most prominent product group was methyl containing ring opening products followed by ring opening products containing propyl groups, such as methyl isopropyl cyclohexane and dimethyl isopropyl cyclopentane.

The selectivities to the desired ROP at the same conversion level of 26 % (Fig. 8, *d*) were for 2 wt.% Ir-H-NK-MM-BE or 2 wt.% Ir-H-NK-MM-TON embedded mesoporous materials about 3 mol.% and 26 mol.%, respectively. This result can be explained by the fact that,

since the reaction rate over the latter catalyst was slower due to the steric limitations, also the extent of the formation of CP was suppressed over 2 wt.% Ir-H-NK-MM-TON compared to the 2 wt.% Ir-H-NK-MM-BE catalyst. It can thus be concluded that due to the smaller pore sizes the selectivity to ROP was 8.7 fold higher for 2 wt.% Ir-H-NK-MM-TON than for 2 wt.% Ir-H-NK-MM-BE embedded material at the conversion level of 26 mol.%. The final selectivity after 1440 min reaction to ROP over the 2 wt. % Ir-H-NK-MM-BE catalyst was, however, about 33 % at the conversion level of 98 %.

High amounts of CP and heavy products were formed after prolonged reaction times (1440 min) over 2 wt.% Ir-H-NK-MM-BE catalyst corresponding to the conversion level of 98 %. The corresponding amounts of CP and heavy products over 2 wt.% Ir-H-NK-MM-TON catalyst after 1440 min were only 3.9 mol.% and below 1 mol.%, respectively, however, the conversion was only 42 %. Additionally the higher yields of ROPs over Ir-H-NK-MM-TON compared to Ir-H-NK-MM-BE can be seen when plotting the ratio between the yields of ROP and the sum of the yields of ROP and CP as a function of conversion (not depicted here). The main difference between 2 wt.% Ir-H-NK-MM-BE embedded mesoporous material and 2 wt.% Ir-H-NK-MM-TON catalyst is, as already been mentioned, the slower reaction rates over the latter catalysts. The formation of CP and heavy products was catalyzed by the presence of strong Brønsted acid sites, medium and strong Lewis acid sites in 2 wt.% Ir-H-NK-MM-TON embedded mesoporous material (Table 1).

3.2.3. Effect of Ir-modification embedded mesoporous material on conversion of decalin and selectivity to ring opening products. The effect of Ir was studied using 2 wt.% Ir-H-NK-MM-TON and H-NK-MM-TON as catalysts (Fig. 9). The decalin conversion over 2 wt.% Ir-H-NK-MM-TON embedded mesoporous material was 1.5 fold higher than that achieved over H-NK-MM-TON embedded mesoporous catalyst at the normalized time of 20 min, as expected (Fig. 9, *a*). The reason for this result is the isomerization, which is the first reaction step and occurs predominantly over metal sites [7]. The conversion at prolonged reaction time of 1440 min was only about

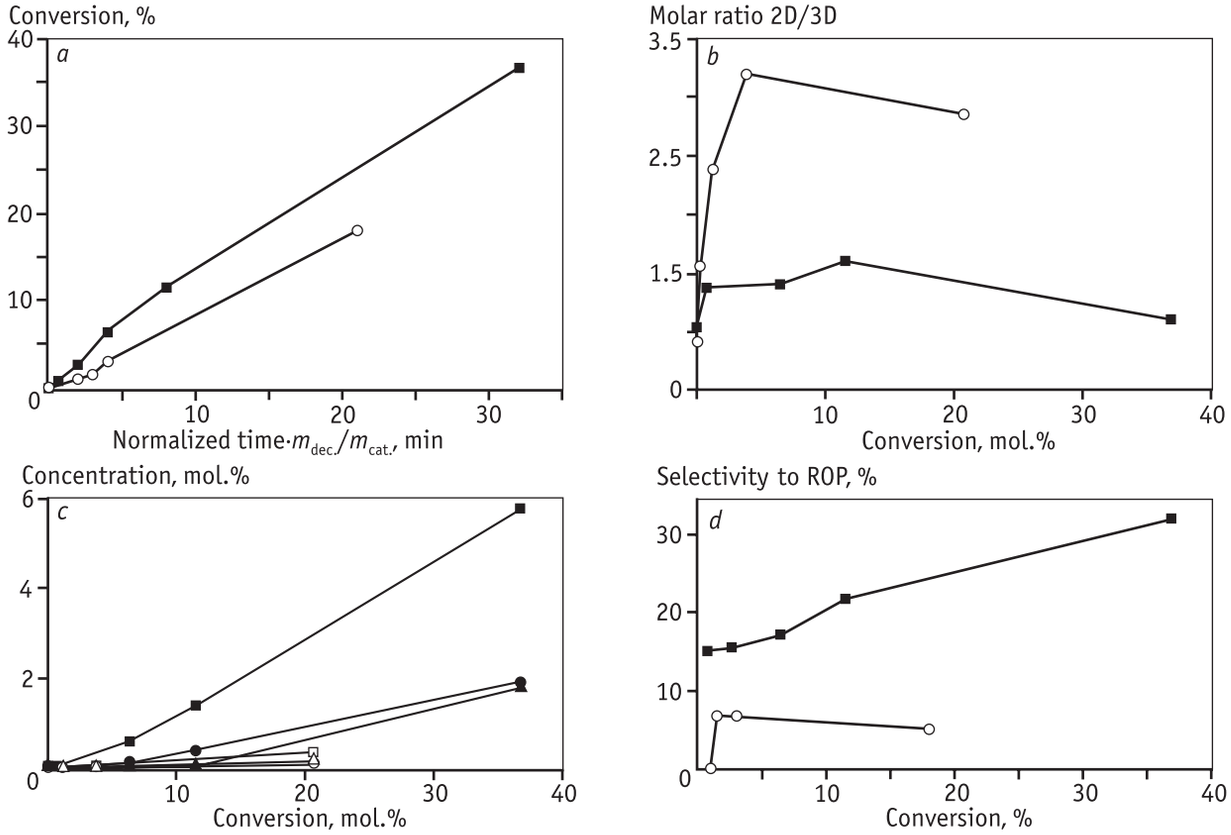

Fig. 9. Effect of Ir on conversion of decalin (*a*), molar ratios of 2D to 3D isomers (*b*), concentration of ROP (*c*) and selectivity to ring opening products as a function of conversion (*d*) in decalin ring opening at 573 K and 6 MPa

Symbols (*a, b, d*): ■ – 2 wt.% Ir-H-NK-MM-TON, ○ – H-NK-MM-TON catalysts

Symbols (*c*): ○ – methyl ROP, □– ethyl ROP, △ – propyl ROP; open symbol – without Ir, solid symbol – with Ir

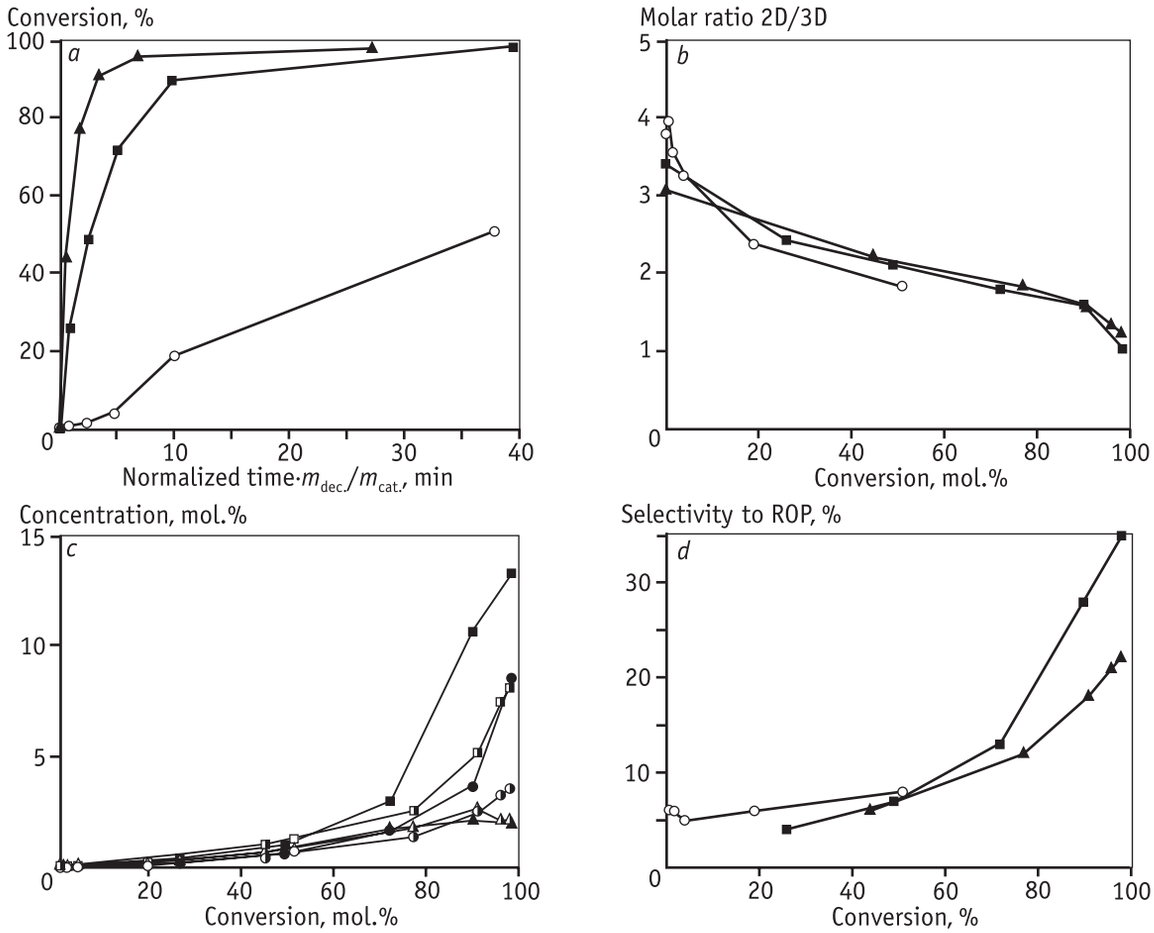

Fig. 10. Effect of temperature on conversion of decalin (*a*), molar ratio of 2D to 3D isomers (*b*), concentration of ROP (*c*) and selectivity to ring opening products as a function of conversion (*d*) during ring opening reaction of decalin over 2 wt.% Ir-H-NK-MM-BE catalyst at 6 MPa

Symbols (*a, b, d*): ▲ – 623K, ■ – 573 K, ○ – 523 K

Symbols (*c*): ○ – methyl ROP, □ – ethyl ROP, △ – propyl ROP; open symbol – 523 K, half-filled – 573 K, solid – 623 K

16 % for H-NK-MM-TON embedded mesoporous material, whereas the corresponding conversion level over the Ir-modified catalyst was 34 % (Fig. 10, *a*). On the other hand, both catalysts were active for a long time and the decalin conversions were continuously increasing over these catalysts with increasing reaction time.

The main products in decalin transformation over the H-NK-MM-TON catalyst were isomers with selectivity increasing from 76 mol.% to 84 mol.% in the conversion range of 1 % to 18 %. The formation rate of isomers was about twice as high over 2 wt.% Ir-H-NK-MM-TON than over H-NK-MM-TON catalyst. Contrary to the results for the H-NK-MM-TON embedded mesoporous material, the isomer selectivity for 2 wt.% Ir-H-NK-MM-TON decreased from 84 to 55 mol.% with increasing decalin conversion from 2 % to 37 %, respectively. The decrease in isomer selectivity is a result of the faster further reactions of isomers over this catalyst than in the isomerization reactions. Similarly to the formation rate of isomers, also the formation rate of ROP was 6.2 fold higher for 2 wt.% Ir-H-NK-MM-TON catalyst than for the metal free catalyst H-NK-MM-TON. The ratio between 2D to 3D isomers in the absence of Ir was maximally about 3.2, whereas this ratio was only about 1.6 in case of 2 wt.% Ir-H-NK-MM-TON embedded mesoporous material (Fig. 9, *b*). After prolonged reaction times the 2D/3D ratio decreased with increasing conversion. Since also in this case the formation of ring opening products was more extensive over Ir-modified catalyst than over the one without Ir (see below), it can be stated that 2D isomers reacted faster further to ring opening products. Both in the absence and presence of Ir the maximum concentrations of 2D and 3D isomers were not reached within the studied reaction time showing that the consecutive reaction path-

way for formation of ring opening products was not very fast.

The formation of different ring opening products over 2 wt.% Ir-H-NK-MM-TON and H-NK-MM-TON embedded mesoporous materials is shown in Fig. 9, *c*. These results are analogous to those presented in the Section 3.2.2 showing that the main products were ethyl ring opening products being maximally two fold the concentration of methyl ROP.

The selectivity to ring opening products over 2 wt.% Ir-H-NK-MM-TON catalyst increased with increasing conversion from 15 mol.% to about 33 mol.% (Fig. 9, *d*). Additionally the benefit of Ir-modification was clearly visible in Fig. 8 showing the ratio between the yield of ROP and the sum of the yields of ROP and COP as a function of conversion. Higher amount of weak acid sites in 2 wt.% Ir-H-NK-MM-TON compared to H-NK-MM-TON catalyst enhanced the formation of ROP. In the third step also the formation rate of CP was 1.8 fold higher with Ir-modified catalyst than with H-NK-MM-TON catalyst. As a consequence of the lower reaction rates over H-NK-MM-TON, the selectivity to ROP remained approximately constant with an increasing conversion, being about 8 mol.% (Fig. 9, *d*). Higher amounts of strong Brønsted and Lewis acid sites in H-NK-MM-TON catalyst compared to 2 wt.% Ir-H-NK-MM-TON embedded mesoporous material, however, increased the final selectivity of CP after 1440 min up to 9 % (Table 3). Thus it can be concluded that due to the slower reaction rates over H-BE catalyst compared to the 2 wt.% Ir-H-NK-MM-TON embedded mesoporous material, a higher selectivity to ROP was achieved over 2 wt.% Ir-H-NK-MM-TON catalyst.

3.2.4. Effect of temperature on conversion of decalin and selectivity to ring opening products over Ir-modified embedded mesoporous material. Higher temperature enhanced the initial decalin transformation rate, as expected

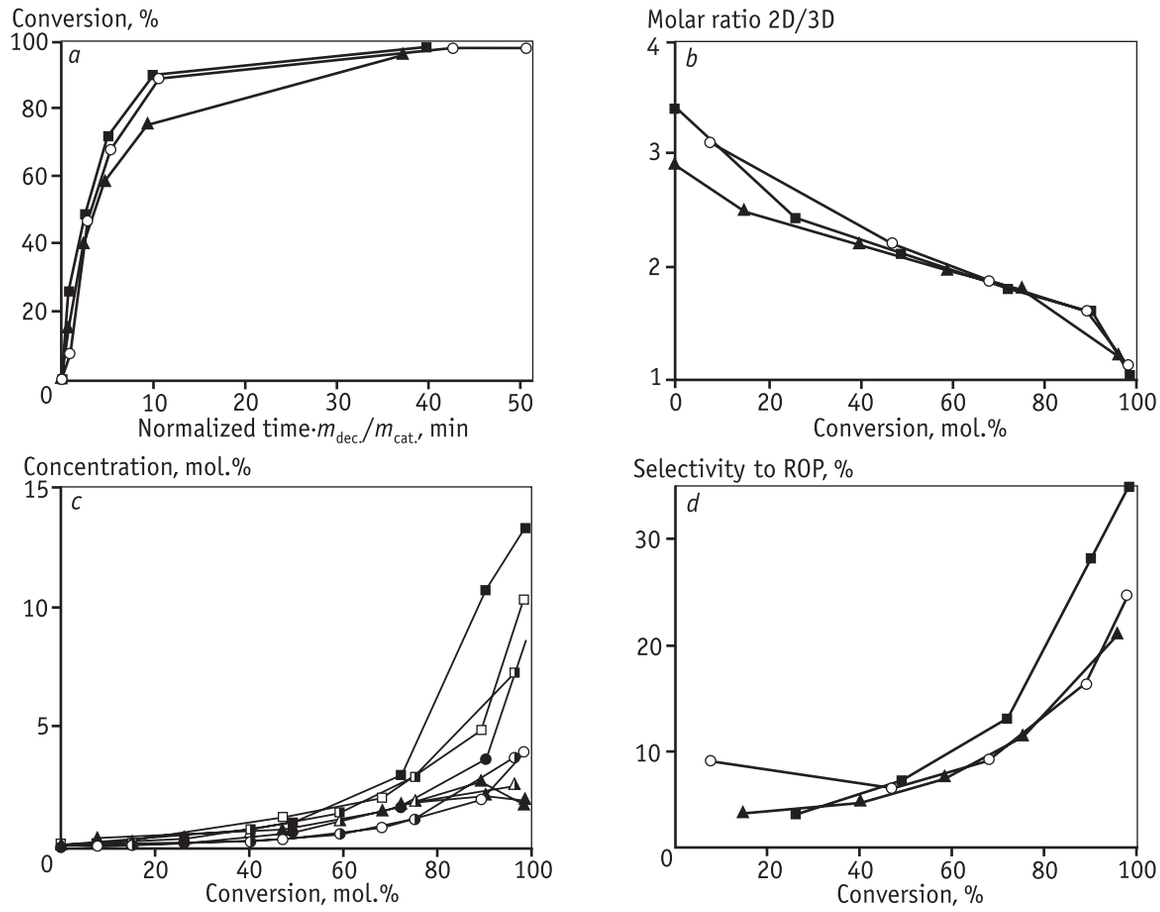

Fig. 11. Effect of pressure on conversion of decalin (*a*), molar ratio of 2D to 3D isomers (*b*), concentration of ROP (*c*) and selectivity to ring opening products as a function of conversion (*d*) during ring opening reaction of decalin over 2 wt.% Ir-H-NK-MM-BE catalyst at 573 K

Symbols (*a, b, d*): ■ – 6 MPa, ○ – 4 MPa, ▲ – 2 MPa
Symbols (*c*): ○ – methyl ROP, □ – ethyl ROP, △ – propyl ROP; solid symbol – 6 MPa, open symbol – 4 MPa, half-filled symbol – 2 MPa

(Fig. 10, *a* and Table 3). It should, however, be pointed out that the final conversions achieved at 573 K and 623 K were quite similar, whereas at 523 K the reaction was much slower, thus only about 28 % conversion was achieved after 20 min normalized time and after 1440 min the conversion was 52 %.

The product distribution was clearly affected by reaction temperature. The formation of isomers was lower at 673 K than at 573 K and 623 K, respectively at 50 % conversion level. However, at high conversions the isomer selectivities were the same at 573 K and at 623 K. On the other hand, the ratio between 2D to 3D isomers was not altered by changing the reaction temperature (Fig. 10, *b*), which might indicate that there are no differences in the activation energies of their formation.

The distribution of different ring opening (namely methyl-, ethyl and propyl-substituted) products is not affected by variation of temperature (Fig. 10, *c*). The main products were ethyl ring opening products, followed by methyl and propyl containing products.

The highest selectivities to ROP were achieved at high conversion levels at 573 K (Fig. 10, *d*). Furthermore, higher ratio between the yield of ROP towards the sum of ROP and CP as a function of conversion were achieved at a lower temperature, 523 K compared to 623 K. These results are in accordance with the trend of obtaining higher amounts of cracking products with an increasing temperature. At 623 K, the formation of heavy products was also enhanced; at 623 K being about 2.4 fold of that achieved at 573 K after 1440 min.

3.2.5. Effect of pressure on conversion of decalin and selectivity to ring opening products over proton form and Ir-modified embedded mesoporous materials. The effect of pressure was investigated by carrying out decalin transformations over 2 wt.% Ir-H-NK-MM-BE catalyst at 573 K and 2, 4, 6 MPa. Slightly higher initial rates were achieved at 6 MPa compared to 2 and 4 MPa (Table 3). The conversion after 20 min at 2 MPa was lower than achieved at 4 MPa and 6 MPa being 80 %, 91 % and 91 %, respectively (Fig. 11, *a*). Thus it can be concluded that decalin transformation proceeded faster at elevated pressures, e. g. at 4 and 6 MPa.

The ratio between the 2D to 3D isomers was not affected by pressure change as can be seen from Fig. 11, *b*. Among ROP products the highest concentration of ethyl ROP products was achieved at 6 MPa (Fig. 11, *c*). The highest selectivity to ROP was achieved at 6 MPa and at 573 K (Fig. 11, *d*). On the other hand, the selectivities to isomers and cracking products were only slightly affected by pressure (Table 3, entries 5—7). At high conversion level, however, the formation of cracking products was somewhat favored at lower pressure, since 38 mol.% of CP were formed at 98 % conversion under 4 MPa, whereas the corresponding value under 6 MPa was 31 %. The formation rates of heavy compounds were also slower under higher pressures compared to lower pressures, since 1.7 fold amounts of heavy compounds were obtained at 4 MPa at 573 K than at 6 MPa, when the conversion level was 98 mol.%. Thus the main conclusions from the effect of pressure are that slightly higher selectivities to ROP were achieved at 6 MPa compared to lower pressures.

4. Conclusions

In this work novel types of Ir-modified embedded mesoporous materials containing MCM-41 structure together with BE and TON zeolites were synthesized and characterized by XRD, SEM, Py-FTIR and TEM. The results revealed that pure BE and TON phases were found in embedded materials together with the mesoporous structure. Furthermore, the structure of the embedded materials remained intact after Ir-introduction. The acidity measurements revealed that there are metal-support interactions affecting the acidities of the studied materials. A narrow Ir-particle size distribution was achieved in mesoporous MCM-41 material embedded with TON zeolite.

In the ring opening of decalin (as a model compound in middle distillates) the effects of support structure, metal and temperature were studied. This process if utilized industrially in a selective manner will improve substantially the cetane number by transforming molecules with two naphthenic rings into linear or mono-branched paraffins.

The results revealed that Ir-modified embedded MCM-41 material containing BE zeolite was very active in this reaction at 573 K under 6 MPa. The maximum selectivity to ring opening products was 31 % at 98 % conversion level. On the other hand, only 37 % conversion was achieved over Ir-modified MCM-41 containing zeolite TON showing clearly the effect of structure on the catalytic performance. The metal modification was beneficial for the decalin conversion when comparing the performances of Ir-modifed embedded MCM-41 material containing TON with the corresponding catalyst without Ir. Furthermore, the selectivity towards ring opening products was more than 2-fold in the presence of Ir than in the absence of it. The main ring opening products observed over Ir-modified embedded mesoporous materials were ethyl-substituted ones. This is to be expected since the mesoporous structures facilitate the formation of larger molecules. To achieve high selectivity to ring opening

products, the optimum temperature was observed at 573 K giving 35 % selectivity at 98 % conversion. On the other hand, lower selectivities to ring opening products were obtained at 623 K due to enhanced formation of isomers, as well as cracked and heavy products. The highest amount of cracking products was obtained at 623 K being 8 % at 30 % conversion. These results demonstrated the benefit of using embedded mesoporous materials in ring opening of decalin.

This work is a part of the activities at Åbo Akademi Process Chemistry Centre within Finnish Centre of Excellence Programme (2005—2011) by Academy of Finland.

References

1. *Beck J.S., Vartuli J.C., Roth W.J., Leonowicz M.E., Kresge C.T., Schmitt K.D., Chu C.T.W., Olson D.H., Sheppard E.W.* // J. Am. Chem. Soc. 1992. Vol. 114. P. 10834—10843.
2. *Chal R., Gérardin C., Bulut M., van Donk S.* // ChemCatChem. 2011. Vol. 3. P. 67—81.
3. *Zhang Y., Dou T., Li Q., Kang S.* // Recent Progress in Mesostructured Materials / Ed. D. Zhao, S. Qiu, Y. Tang, C. Yu. Elsevier, 2007. P. 491—494.
4. *Guo W., Xiong C., Huang L., Li Q.* // J. Mater. Chem. 2001. Vol. 11. P. 1886—1890.
5. Patent WO 2006/070073. Catalytic materials and method for the preparation thereof / Kumar N., Tiitta M., Salmi T., Österholm H. Pub. date 06.07.2006.
6. *McVicker G.B., Daage M., Touvelle M. S., Hudson C.W., Klein D.P., Baird W.C., Cook B.R., Chen J.G., Hantzer S., Vaughan D.E.W., Ellis E.S., Feeley O.C.* // J. Catal. 2002. Vol. 210. P. 137—148.
7. *Kubicka D., Kumar N., Mäki-Arvela P., Tiitta M., Niemi V., Karhu H., Salmi T., Murzin D.Yu.* // J. Catal. 2004. Vol. 227. P. 313—327.
8. *Kubicka D., Kumar N., Mäki-Arvela P., Tiitta M., Venäläinen T., Salmi T., Murzin D.Yu.* // Stud. Surf. Sci. Catal. 2005. Vol. 158. P. 1669—1676.
9. *Kubicka D., Kumar N., Mäki-Arvela P., Tiitta M., Niemi V., Salmi T., Murzin D.Yu.* // J. Catal. 2004. Vol. 222. P. 65—79.
10. *Kubicka D., Kumar N., Venäläinen T., Karhu H., Kubickova I., Österholm H., Murzin D.Yu.* // J. Phys. Chem. B. 2006. Vol. 110. P. 4937—4946.
11. *Rabl S., Haas A., Santi D., Flego C., Ferrari M., Calemma V., Weitkamp J.* // Appl. Catal. A: Gen. 2011. Vol. 400. P. 131—141.
12. *Weitkamp J., Rabl S., Haas A., Santi D., Ferrari M., Calemma V.* // DGMK Tagungsbericht. 2010. Vol. 3. P. 77.
13. *Mouli K.C., Sundramurthy V., Dalai A.K., Ring Z.* // Appl. Catal. A: Gen. 2007. Vol. 321. P. 17—26.
14. *Mouli K.C., Sundramurthy V., Dalai A.K.* // J. Mol. Catal. A: Chem. 2009. Vol. 304. P. 77—84.
15. *Hernandez-Huseca R., Merida-Robles J., Maireles-Torres P., Rodriguez-Castellon E., Jimenez-Lopez A.* // J. Catal. 2001. Vol. 203. P. 122—132.
16. *Kangas M., Kubicka D., Salmi T., Murzin D.Yu.* // Top. Catal. 2010. Vol. 53. P. 1172—1175.
17. *Kubicka D., Kumar N., Mäki-Arvela P., Tiitta M., Salmi T., Murzin D.Yu.* // Catalysis in Organic Reactions. 2005. P. 279—292.
18. *D'Ippolito S.A., Benitez V.M., Reyes P., Rangel M.C., Pieck C.L.* // Catal. Today. 2011. Vol. 172. P. 177—182.
19. *Moraes R., Thomas K., Thomas S., Van Donk S., Grasso G., Gilson J.-P., Houalla M.* // J. Catal. 2012. Vol. 286. P. 62—77.
20. *Kumar N., Kubicka D., Heikkilä T., Karhu H., Tiitta M., Salmi T., Murzin D.Yu.* // Nanocatalysis / Ed. D.Yu. Murzin. Trivandrum (Kerala, India): Research Signpost, 2006. P. 33—50.
21. *Ardakani S.J., Smith K.J.* // Appl. Catal. A: Gen. 2011. Vol. 403. P. 36—47.
22. *Emeis C.A.* // J. Catal. 1993. Vol. 141. P. 347—354.
23. *Zhou W., He D.* // Catal. Lett. 2009. Vol. 127. P. 437.
24. *Matsukata M., Ogura M., Osaki T., Kikuchi E., Mitra A.* // Microp. Mesop. Mater. 2001. Vol. 48. P. 23—29.
25. Atlas of Zeolite Framework Types / Eds. C. Baerlocher, L. McCusker, D. Olson. 6th ed. Elsevier, 2007. P. 230, 334.

РАСКРЫТИЕ ЦИКЛОВ В ДЕКАЛИНЕ С ИСПОЛЬЗОВАНИЕМ ИРИДИЙСОДЕРЖАЩИХ ГИБРИДНЫХ ЦЕОЛИТНЫХ МЕЗОПОРИСТЫХ МАТЕРИАЛОВ

© 2013 г. **Н. Кумар, П. Маки-Арвела, Н. Мусакка, Д. Кубикка, М. Кангас, М. Тиитта, Х. Остерхольм, А.-Р. Леино, К. Кордас, Т. Хейккила, Т. Салми, Д.Ю. Мурзин**

Производство дизельного топлива с наименьшим негативным влиянием на окружающую среду является одной из важнейших задач современной нефтепереработки. Нефтеперерабатываюшие компании заинтересованы в снижении содержания серы и ароматики в средних дистиллятах. Недостаточно высокое цетановое число может быть увеличено за счет гидрирования и раскрытия циклов сопряженных нафтеновых колец в линейные или моноразветвленные продукты. При этом если гидрирование ароматики осуществить довольно просто, то селективное раскрытие циклов без значительного крекинга представляет собой сложную задачу.

В данной работе были приготовлены гибридные микро-мезопористые материалы на основе MCM-41 совместно со структурами BE или TON. Образцы охарактеризованы различными физико-химическими методами (рентгеновская фотоэлектронная спектроскопия, туннельная и сканирующая электронная микроскопия, ИК-спектроскопия адсорбции с использованием пиридина в качестве зонда) и протестированы в реакции раскрытия циклов в декалине при 523–623 K. Обе фазы, соответствующие микро-мезопористым материалам, присутствовали в приготовленных гибридных материалах. Введение иридия не влияло на фазовую чистоту, изменяя, однако, кислотность из-за взаимодействия металл–носитель. Узкое распределение частиц иридия по размерам было получено в случае встраивания в MCM-41 цеолита структуры TON.

Результаты показали, что модифицированный иридием мезопористый MCM-41 со встроенной структурой цеолита BE активен в раскрытии циклов в декалине при 573 K и 6 МПа. Максимальная селективность по продуктам раскрытия циклов в этом случае составила 31 % при конверсии 98 %. Аналогичного типа материал, но со встроенной структурой цеолита TON, продемонстрировал существенно меньшую активность, что свидетельствует о влиянии структуры носителя на каталитические свойства. Модификация иридием также улучшила конверсию по сравнению с аналогичными катализаторами, не содержащими металла. Кроме того, в присутствии иридия и селективность по продуктам раскрытия циклов оказалась в два раза выше. Детальный анализ 2D/3D изомеров показал, что основные продукты раскрытия циклов на гибридных иридиевых катализаторах содержат в боковой цепи этильную группу.

Повышение температуры приводит к увеличению выхода продуктов крекинга, а также тяжелых углеводородов.

Полученные результаты показывают перспективность использования гибридных микро-мезопористых материалов, содержащих иридий, для проведения реакции раскрытия циклов в декалине, модельном соединении средних дистиллятов.